Peculiar dynamical properties of plutonium hydrides*

MENG Daqiao[1,2], ZHU Zhenghe[1]**, LUO Deli[1,2] and JIANG Gang[1]

(1. Institute of Atomic and Molecular Physics, Sichuan University, Chengdu 610065, China; 2. National Key Laboratory of Surface Physics and Chemistry, Mianyang 621907, China)

Received June 1, 2005; revised August 18, 2005

Abstract In the present work, the structure and spectra of PuH and PuH_2 are defined by B3LYP/SDD method, from which the analytic potential energy function of PuH_2 is derived. The analysis of quasi-classical molecular reaction dynamics is performed to study the state-state process of $Pu(^7F_g) + H_2(X^1\Sigma_g^+)$. It is found that the reaction $Pu(^7F_g) + H_2(X^1\Sigma_g^+) \rightarrow PuH_2(\tilde{X}^7B_1)$ has no threshold. The simultaneous hydrogenation process of plutonium with the main product of PuH_2 is theoretically proved for the first time.

Keywords: hydrogenation reaction of plutonium, molecular dynamics, density functional theory.

The electronic configuration for plutonium atom is KLMN $5s^25p^65d^{10}6s^26p^65f^67s^2$, with six 5f electrons at the transitional border from delocalization to localization. Therefore, the atomic volume of α-Pu is anomalously larger than that of α-Np, which has been a continuous challenge for theoretical explanation[1]. The 5f electrons are assumed to be of itinerant nature, which causes a smaller binding energy[2] than that of 5d. In addition, the hybridized orbital contributed by 5f electrons is much higher, for example, the contributions[3] are 1.932 and 2.578 for the linear orbital sp and sf, and 2.923 and 3.570 for d^2sp^3 and d^2sf^3, respectively. Because of the very small first ionization potential of Pu, i.e. 6.063 eV[4], the charge contribution of double positive cation PuO^{2+} is Pu^+ and O^+ rather than Pu^{2+} and O, and the cases for PuH^{2+} and PuN^{2+} are similar[5].

Plutonium hydrides (PuH and PuH_2) have peculiar dynamical properties due to their special atomic structures. Plutonium reacts with hydrogen at an astonishing rate that never occurs in other metals[6,7]. For example, the activity energy[8] of hydrogenation of ethylene under nickel, palladium and platinum catalysts is about 2.63 kJ/mol, but the activation energy for the processes of hydrogenation of plutonium is nearly zero. Moreover, the reaction of hydrides-coated plutonium with air at room temperature is 10^7—10^8 times faster than that of normal air oxidation of pure plutonium[7]. It is obvious that there is an intrinsic connection between the structure of plutonium and its compounds.

In order to study the dynamical properties of plutonium hydrides, we have to calculate the molecular structure of plutonium hydrides first, and then we can obtain their analytic potential energy functions. Density functional theory (DFT) has been used to calculate the molecular structures of Pu_2, Pu_3 and Pu_4[9,10] in which the various energy terms are expressed by the physical observable electron density based on the Hohenberg and Kohn theorems[11].

The full electron calculation of actinides is time-consuming. The atomic property depends mainly on the valence electrons, so it is possible to use the theory of effective core potential (ECP) or relativistic effective core potential (RECP), in which the atomic core and valence orbital are corrected by Cowan-Griffin Hartree-Fock equation, and the terms of "mass-velocity", "Darwin" and spin-orbital coupling[12] are also considered. These methods have been successfully used to calculate the molecular structure, such as UO_2 and PuO, etc.

1 Molecular potential energy function

1.1 Density functional theory (DFT)

In DFT, electronic energy E is divided into several components,

$$E = E^T + E^V + E^J + E^{XC}, \quad (1)$$

where E^T is the electronic kinetic energy, E^V the po-

* Supported by National Natural Science Foundation of China (Grant No. 10176017) and National Key Laboratory of Surface Physics and Chemistry (Grant No. 04H683)

** To whom correspondence should be addressed. E-mail: Zhuxm@scu.edu.cn

tential energy including the electron-nucleus attraction and nucleus-nucleus repulsion, E^J the electron-electron repulsion, and E^{XC} the exchange-correlation. Except for nucleus-nucleus repulsion, each term can be expressed as the function of electron density ρ

$$E^J = \frac{1}{2}\iint \rho(\boldsymbol{r}_1)(\Delta r_{12})^{-1}\rho(\boldsymbol{r}_2)\mathrm{d}\boldsymbol{r}_1\mathrm{d}\boldsymbol{r}_2, \quad (2)$$

$$E^{XC}(\rho) = \int f(\rho_\alpha(\boldsymbol{r}), \rho_\beta(\boldsymbol{r}), \nabla\rho_\alpha(\boldsymbol{r}), \nabla\rho_\beta(\boldsymbol{r}))\mathrm{d}^3\boldsymbol{r}, \quad (3)$$

$$E^{XC}(\rho) = E^X(\rho) + E^C(\rho), \quad (4)$$

where all the three terms are the functions of electron density. $E^X(\rho)$ and $E^C(\rho)$ are the exchange and correlation functional, respectively. The former is a local functional and only related with the electron density, and the latter is a gradient-corrected functional related with the electron density and its gradient $\nabla\rho$. In 1988, Becke[13] derived the local exchange functional as follows:

$$E^X_{\text{Becke88}} = E^X_{\text{LDA}} - \gamma\int \frac{\rho^{4/3}x^2}{(1 + 6\gamma\sinh^{-1}x)}\mathrm{d}^3\boldsymbol{r}, \quad (5)$$

$$E^X_{\text{LDA}} = -\frac{3}{2}\left(\frac{3}{4\pi}\right)^{1/3}\int\rho^{4/3}\mathrm{d}^3\boldsymbol{r}, \quad (6)$$

where ρ is a function of $\boldsymbol{r}$, $x = \rho^{-4/3}|\nabla\rho|$, γ is a parameter fitted with the exchange energy of noble atoms ($\gamma = 0.0042$ a.u.). Similarly, in 1992, Perdew and Wang[14] suggested a corrected functional:

$$E^C = \int\rho\varepsilon_C(r_s(\rho(\boldsymbol{r})), \zeta)\mathrm{d}^3\boldsymbol{r}, \quad (7)$$

where

$$r_s = \left[\frac{3}{4\pi\rho}\right]^{1/3}, \quad \zeta = \frac{\rho_\alpha - \rho_\beta}{\rho_\alpha + \rho_\beta},$$

$$\varepsilon_C(r_s, \zeta) = \varepsilon_C(\rho, 0) + a_C(r_s)\frac{f(\zeta)}{f''(0)}(1 - \zeta^4) + [(\varepsilon_C(\rho, 1) - \varepsilon_C(\rho, 0))]f(\zeta)\zeta^4,$$

$$f(\zeta) = \frac{[(1 + \zeta)^{4/3} + (1 - \zeta)^{4/3} - 2]}{(2^{4/3} - 2)}.$$

Here r_s is the density parameter and ζ the correlated spin polarization. DFT is a joint calculation with the exchange and correlation functional. The B3LYP method used in the present work is to combine Becke's exchange functional and the correlated functional of Lee, Yang and Parr, both being gradient-corrected. The local correlation functional is from Vosko, Wilk and Nusair (VWN). Then the so-called Becke's three parameter functional[15] is

$$E^{XC}_{\text{B3LYP}} = E^X_{\text{LDA}} + c_0(E^X_{\text{HF}} - E^X_{\text{LDA}}) + c_X\Delta E^X_{\text{B88}} + E^C_{\text{VWN3}} + c_C(E^C_{\text{LYP}} - E^C_{\text{VWN3}}). \quad (8)$$

Using the G1 method, Becke has obtained: $c_0 = 0.20$, $c_X = 0.72$ and $c_C = 0.81$ by optimizing exchange and correlation energy. Eq. (8) will be used for the presented DFT-SCF calculations.

1.2 Structures of PuH and PuH_2

The electronic configuration of plutonium atom is (Rn) $5f^67s^2$, and its 60 of core electrons ($1s^22s^22p^63s^23p^63d^{10}4s^24p^64d^{10}4f^{14}$) can be represented by relativistic effective core potential (RECP)[16], and the 34 of valence electrons ($5s^25p^65d^{10}6s^26p^65f^67s^2$) are used for the calculations. The calculated results are quite reasonable based on the RECP/SDD and DFT theories.

From the ground states ^7F_g of plutonium and ^2S_g of hydrogen H, it is possible to form the 4, 6 and 8-multiplicity of PuH. All of the possible multiplicities have been optimized by B3LYP/SDD, and their ground state PuH($X^8\Sigma$) is listed in Table 1.

Table 1. Potential energy parameters and spectroscopic data of PuH($X^8\Sigma$)

D_e(eV)	R_e(nm)	a_1(nm^{-1})	a_2(nm^{-2})	a_3(nm^{-3})		
1.8029	0.21105	26.0351	173.8361	479.0386		
f_2(0.1 fJ·nm^{-2})	f_3(fJ·nm^{-3})	f_4(10 J·nm^{-4})	ω_e(cm)	$\omega_e\chi_e$(cm)	B_e(cm)	α_e(cm)
0.9537	-3.1815	7.6174	1274.90	22.345	3.8021	9.1592×10^{-2}

Using the B3LYP/SDD method, the full potential curve of the ground state PuH ($X^8\Sigma$) is calculated, and based on the normal equations, the calculated results are fitted to the Murrell-Sorbie function form

$$V = -D_e(1 + a_1\rho + a_2\rho^2 + a_3\rho^3)\exp(-a_1\rho), \quad (9)$$

where $\rho = r - r_e$; r, r_e are the inter-nuclei distance and its equilibrium value, respectively; D_e, a_1, a_2, a_3 are the fitted coefficients (Table 1).

Fig. 1 shows the calculated and fitted molecular potential energies of PuH($X^8\Sigma$). The two curves agree well with each other. Based on the Murrell—Sorbie potential energy function, the force and spectroscopic constants for PuH($X^8\Sigma$) were calculated[17] (see Table 1).

For the possible 5, 7 and 9 multiplicities of PuH_2, its ground state by optimization is $PuH_2(\tilde{X}^7B_1)$. In order

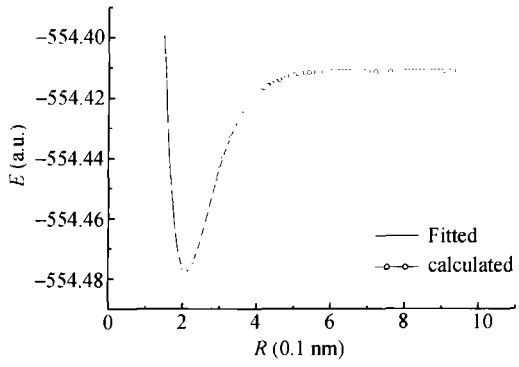

Fig. 1. Molecular potential energy curve of PuH($X^8\Sigma$).

to calculate the potential energy function and spectroscopic constants, we have to determine the dissociation energy D_e of $PuH_2(\tilde{X}^7B_1)$ based on the dissociation limit $PuH_2(\tilde{X}^7B_1) \rightarrow Pu(^7F_g) + 2H(^2S_g)$. The dissociation energy $D_e = E(Pu) + 2E(H) - E(PuH_2) = 4.469881217$ eV, where the optimized $E(Pu)$, $E(H)$ and $E(PuH_2)$ are -553.9044258, -0.502257 and -555.0732012 a.u., respectively. Table 2 lists all the parameters.

Table 2. Structural and spectroscopic parameters for $PuH_2(\tilde{X}^7B_1)$

	Present work	Ref. [18]
Structure	$R_{PuH} = 0.20372$ nm, $\angle HPuH = 104.9236°$	$R_{PuH} = 0.20368$ nm, $\angle HPuH = 105.139°$
Harmonic frequency	$\upsilon_1 = 1304.7718\ cm^{-1}$, $\upsilon_2 = 512.5435\ cm^{-1}$, $\upsilon_3 = 1451.4252\ cm^{-1}$	
Dissociation energy	4.46988 eV	4.4736 eV
Force constants ($aJnm^{-2}$)	$f_{11}(HPu) = 0.0725225$, $f_{22}(PuH) = 0.0724700$, $f_{12} = -7.80447 \times 10^{-3}$, $f_{13} = -8.83482 \times 10^{-4}$, $f_{23} = -8.98740 \times 10^{-4}$, $f_{33}(\angle HPuH) = 0.0739787$	

1.3 Many-body expansion theory[17,19] and potential energy function of PuH_2

The potential energy function for PuH_2 can be written as

$$V(R_1, R_2, R_3) = V^{(2)}_{PuH}(R_1) + V^{(2)}_{PuH}(R_2) + V^{(2)}_{HH}(R_3) + V^{(3)}_{HPuH}(R_1, R_2, R_3), \quad (10)$$

where $R_1 = R_2 = R_{PuH}$, $R_3 = R_{HH}$. The two-body term in Eq. (10) is Murrell-Sorbie function (9). The data of $V^{(2)}_{PuH}(R_2)$ is shown in Table 1, and the potential energy function of $H_2(X^1\Sigma_g^+)$ is quoted from Ref. [17] and shown in Table 3.

Table 3. Two-body term parameters of $H_2(X^1\Sigma_g^+)$[17]

	D_e(eV)	R_e(nm)	$A_1(nm^{-1})$	$a_2(nm^{-2})$	$a_3(nm^{-3})$
$H_2(X^1\Sigma_g^+)$	4.747	0.07414	39.61	406.4	3574.0

Considering the symmetry, the suitable reference coordinates should be selected to express a given potential energy function. Here, take the C_{2v} configuration as a reference coordinate of PuH_2, i.e. $R_1^\circ = R_2^\circ = R_{PuH}^\circ = 0.203722$ nm and $R_3^\circ = 0.323082$ nm. Then the inner coordinates are

$$\rho_i = R_i - R_i^\circ, \quad (i = 1, 2, 3).$$

Correspondingly, their symmetrical inner coordinates are expressed as a matrix equation

$$\begin{bmatrix} S_1 \\ S_2 \\ S_3 \end{bmatrix} = \begin{bmatrix} 1 & 0 & 0 \\ 0 & 1/\sqrt{2} & 1/\sqrt{2} \\ 0 & 1/\sqrt{2} & -1/\sqrt{2} \end{bmatrix} \begin{bmatrix} \rho_1 \\ \rho_2 \\ \rho_3 \end{bmatrix}, \quad (11)$$

and $V^{(3)}_{PuH_2}(R_1, R_2, R_3)$ in Eq. (10) is a three-body term expressed as

$$V^{(3)}_{HpuH}(R_1, R_2, R_3) = P \cdot T, \quad (12)$$

where P is a polynomial expressed as the symmetrical inner coordinate S_i, and T the range function. The functional form is as follows:

$$P = C_0 + C_1S_1 + C_2S_2 + C_3S_2^2 + C_4S_3^2 + C_5S_1S_2 + C_6S_3^4 + C_7S_1^2 + C_8S_1(S_2^2 + S_3^2) + C_9S_2S_3^2, \quad (13)$$

and

$$T = [1 - \tanh(\gamma_1S_1/2)][1 - \tanh(\gamma_2S_2/2)] \cdot [1 - \tanh(\gamma_3S_3/2)]. \quad (14)$$

In Eqs. (13) and (14), there are 10 linear coefficients C_0, C_1, C_2, C_3, C_4, C_5, C_6, C_7, C_8, and C_9, and 3 non-linear coefficients γ_1, γ_2 and γ_3. The linear coefficients are determined from the known conditions (Table 2) and the non-linear coefficients can be defined by optimal calculations. Table 4 lists all the coefficients, and Figs. 2 and 3 show the potential energy contour.

Table 4. All the linear and non-linear coefficients for $PuH_2(\tilde{X}^7B_1)$

C_0	C_1	C_2	C_3	C_4	C_5	C_6	C_7	C_8	C_9	
-4.384847×10^{-1}	2.855640×10^{-1}	-9.148243×10^{-1}	-1.515451419	$-3.988296^1 \times 10^{-1}$	$-3.748360^1 \times 10^{-1}$	2.471955×10^{-1}	1.176774×10^{-1}	-4.326033×10^{-1}	1.0511264×10^{-2}	$\gamma_1 = 1.2$, $\gamma_2 = 3.5$, $\gamma_3 = 1.2$

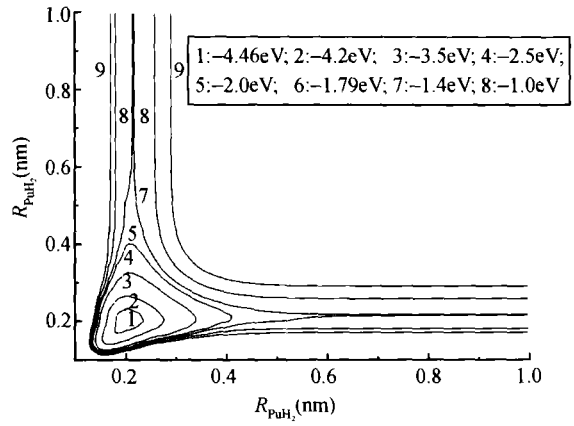

Fig. 2. Bond stretching contours for PuH_2.

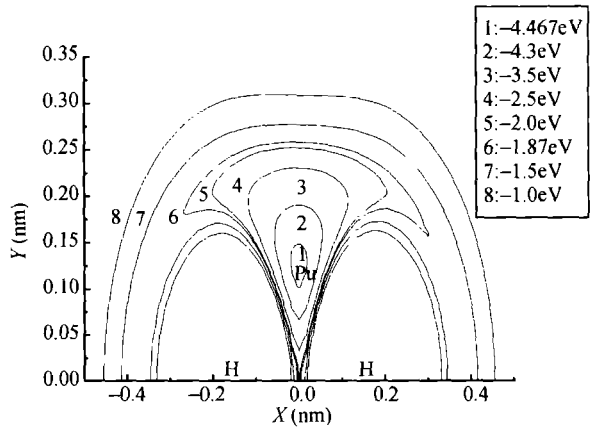

Fig. 3. Contours for the movement of Pu around H-H. R_{HH} = 0.32308 nm, origin$(X, Y) = (0, 0)$.

Using the B3LYP/SDD method, the derived analytic potential energy function of PuH_2 is expressed by Eqs. (11)—(14) and displayed as the contour maps in Figs. 2 and 3. The equilibrium geometry ($R_{PuH} = 0.203722$ nm) and the depth of potential trap (4.46988 eV) are fairly demonstrated in Fig. 2, and no saddle points are shown on two equivalent reactive channels $Pu + H_2 \rightarrow PuH_2$. Therefore, it is a reaction without threshold energy. Fig. 3 shows the energy contours of the potential for a Pu atom moving around an H-H group whose bond length is $R_{HH} = 0.32308$ nm fixed at the X coordinate. It also fairly illustrates the structural characteristic of PuH_2 (X^7B_1), which provides the fundamental data for the dynamics of PuH_2 system. Next, we will study the molecular dynamics for the reactive process $Pu(^7F_g) + H_2(X^1\Sigma_g^+)$.

2 Molecular reaction dynamics[20,21]

2.1 Motion equation for triatomics

In the center of mass coordinate system for the triatomic system, we can set up a set of 12 equations under the analytic potential energy function of PuH_2 expressed as internal coordinates (R_1, R_2, R_3),

$$\begin{cases} \dot{Q}_j = \dfrac{1}{\mu_{BC}} P_j, \quad (j = 1,2,3), \\ \dot{Q}_j = \dfrac{1}{\mu_{A,BC}} P_j, \quad (j = 4,5,6), \\ -\dot{P}_j = \dfrac{1}{R_{AB}} \cdot \dfrac{m_C}{m_B + m_C} \cdot \left(\dfrac{m_C}{m_B + m_C} Q_j + Q_{j+3} \right) \\ \quad \cdot \dfrac{\partial V(R_{AB}, R_{BC}, R_{CA})}{\partial R_{AB}} + \dfrac{\dot{Q}_j}{R_{AB}} \\ \quad \cdot \dfrac{\partial V(R_{AB}, R_{BC}, R_{CA})}{\partial R_{BC}} + \dfrac{1}{R_{CA}} \\ \quad \cdot \dfrac{m_C}{m_B + m_C} \cdot \left(\dfrac{m_C}{m_B + m_C} Q_j - Q_{j+3} \right) \\ \quad \cdot \dfrac{\partial V(R_{AB}, R_{BC}, R_{CA})}{\partial R_{CA}}, \quad (j = 1,2,3), \\ -\dot{P}_j = \dfrac{1}{R_{AB}} \cdot \left(\dfrac{m_C}{m_B + m_C} Q_j + Q_{j+3} \right) \\ \quad \cdot \dfrac{\partial V(R_{AB}, R_{BC}, R_{CA})}{\partial R_{AB}} \\ \quad - \dfrac{1}{R_{CA}} \cdot \left(\dfrac{m_C}{m_B + m_C} Q_j - Q_{j+3} \right) \\ \quad \cdot \dfrac{\partial V(R_{AB}, R_{BC}, R_{CA})}{\partial R_{CA}}, \quad (j = 4,5,6). \end{cases} \tag{15}$$

Eq. (15) is a set of equations of the motion for triatomics ABC under the analytic potential energy hyper-surface $V(R_{AB}, R_{BC}, R_{CA})$, and its numerical solution can give the trajectory of motion, from which the reactive cross section and threshold energy, etc., can be calculated.

For the given initial conditions, the set of equations (15) have been numerically solved using the combined Runge-Kutta-Gill (RKG) method and Adms-Moulton (AM) method with the program written by our research group.

For the reactions $A + BC \rightarrow AB + C$ and $A + BC \rightarrow ABC$, based on about 20000 trajectories, the reaction probability P and reactive cross section σ_r are expressed as

$$P(E_t, V, J, b) = \lim_{N \to \infty} \frac{N_r(E_t, V, J, b)}{N(E_t, V, J, b)}, \tag{16}$$

$$\sigma_r(E_t, V, J) = 2\pi \int_0^{b_{max}} P(E_t, V, J, b) b db = \pi b_{max}^2 \lim_{N \to \infty} \frac{N_r(E_t, V, J)}{N(E_t, V, J)}, \tag{17}$$

where b_{max} is a maximum impact parameter defined as the possible maximum collision distance allowed for the activated reaction; N and N_r are the total and reactive trajectories, respectively; E_t is the relative collision kinetic energy; V and J are the vibration and rotational quantum number, respectively.

The distributions of the given vibration V and rotational energy J levels for products AB, BC and AC of the reactions A + BC→AB + C, A + BC→A + BC and A + BC→AC + B are given by the trajectory numbers, i.e. the distribution of the particle number of products.

For a given kinetic energy E_t, there is a maximum impact parameter b_{max}, and its value is chosen as a boundary value at which the elastic collision is just transited to inelastic collision for a given reaction. The reactive trajectory N_r will be counted for a given reaction from the total N trajectories.

2.2 Quasiclassical molecular reaction dynamics for PuH_2 system

The present work calculates all the processes of reaction $Pu(^7F_g) + H_2(X^1\Sigma_g^+)$ using the quasiclassical Monte-Carlo trajectory method, and tries to evaluate the possible mechanism for plutonium corrosion.

The initial kinetic energies E_t of Pu atom are taken as 4.184, 41.84, 83.68, 209.2, 251.04, 292.88, 418.4, 627.6, 836.8, 1046.0 and 1255.2 kJ/mol, respectively; the other initial parameters, such as R_{HH}, ρ (the distance between H_2 and Pu) and the orientation angles(θ, ψ, η) are randomly chosen by Monte-Carlo method. The impact parameter b is uniformly distributed between 0 and b_{max}^2. The initial vibration quantum number of ground state $H_2(X^1\Sigma_g^+)$ is zero, and the initial distance between the mass center and Pu atom is taken as ρ = 2 nm. We use General Trajectory Program to calculate the dynamics of reaction $Pu + H_2(X^1\Sigma_g^+)$, and find 5 channels[22] for the collision system $Pu(^7F_g) + H_2(X^1\Sigma_g^+)$:

$$Pu(^7F_g) + H_2(X^1\Sigma_g^+) \rightarrow \begin{cases} PuH(X^8\Sigma) + H(^2S_g) & \text{Channel 1,} \\ Pu(^7F_g) + H_2(X^1\Sigma_g^+) & \text{Channel 2,} \\ PuH(X^8\Sigma) + H(^2S_g) & \text{Channel 3,} \\ PuH_2(\tilde{X}^7B_1) & \text{Channel 4,} \\ Pu(^7F_g) + 2H(^2S_g) & \text{Channel 5.} \end{cases} \quad (18)$$

Based on the analytic potential energy function of PuH_2, the set of 12 equations for (15) can be set up, so, all the collision trajectories for system $Pu + H_2(X^1\Sigma_g^+)$ have been calculated and analyzed. The distributed products for each channel with the initial kinetic energy E_t are listed in Table 5.

Table 5. The distribution of products for $Pu + H_2(X^1\Sigma_g^+)$

E_t(kJ·mol^{-1})	b_{max}(nm)	Channel				
		1	2	3	4	5
4.18	0.68		9725		9778	
41.84	0.54		16505		3279	
83.68	0.50		19525		440	
209.20	0.44		19991		9	
251.04	0.11	2	19992	1	4	
292.88	0.16	949	18090	961		
418.40	0.24	735	18304	961		
627.60	0.25	262	18440	372		926
836.80	0.24	100	18120	60		1720
1046.00	0.23	40	17969	27		1964
1255.20	0.22	13	17826	7		2154

For given v, j and b, the reaction probability P and reactive cross section σ_r are calculated by Eqs. (16) and (17) for the complex channel (PuH_2) and exchange reaction channel $Pu(^7F_g) + HH'(v = j = 0) \rightarrow PuH + H$. Table 6 lists the cross section for complex compound, and Table 7 gives the cross section for exchange reaction $Pu + H_2 \rightarrow PuH + H$, and all the cross sections are plotted in Fig. 4.

Table 6. The cross section for $Pu + H_2 \rightarrow PuH_2$

E_t(kJ·mol^{-1})	4.184	41.84	83.68	209.20	251.04
b_{max}(nm)	0.68	0.54	0.50	0.44	0.11
σ_r(nm^2)	0.710212	0.150193	0.01727876	0.000274	7.6E-06

Table 7. The cross section for $Pu + H_2 \rightarrow PuH + H$

E_t(kJ·mol^{-1})	251.04	292.88	418.4	627.6	836.8	1046	1255.2
b_{max}(nm)	0.11	0.16	0.24	0.25	0.24	0.23	0.22
σ_r(10^{-3} nm^2)	5.7E-06	7.68E-03	1.535E-02	6.22E-03	1.45E-03	5.6E-04	1.5E-04

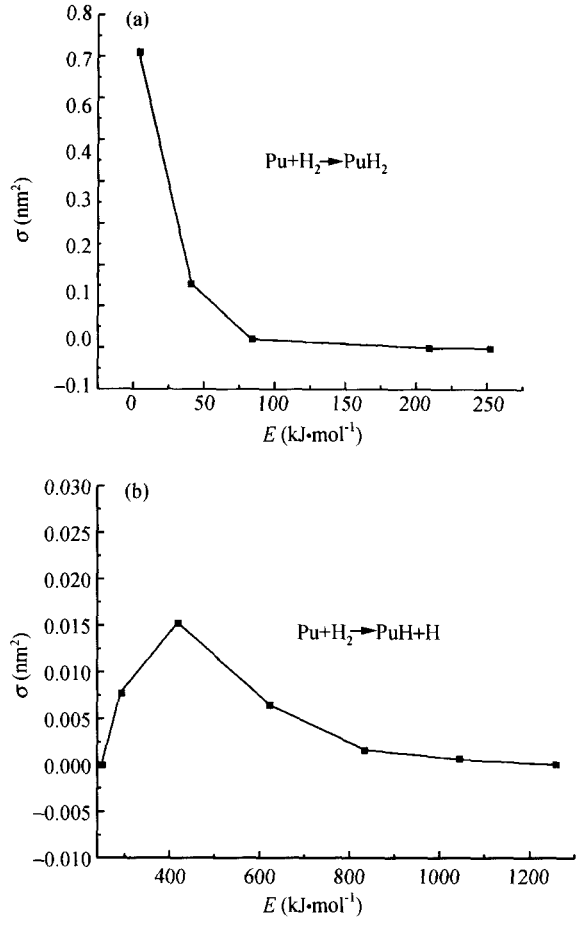

Fig. 4. The cross section versus the collison kinetic energy for the complex (a) and exchange (b) reactions.

From Tables 6, 7 and Fig. 4, it is obvious that the cross section of reaction $Pu + H_2 \rightarrow PuH_2$ descends with the ascent of the initial kinetic energy when E_t is less than 251.04 kJ/mol. Therefore, the complex reaction has no threshold. However, when the initial kinetic energy E_t is within 251.0—836.8 kJ/mol, the exchange reaction $Pu + H_2 \rightarrow PuH + H$ will occur, and it has a threshold. There is a maximum for the cross section within 251.04—836.8 kJ/mol of the initial kinetic energy E_t due to the competition of reaction $Pu + H_2 \rightarrow PuH + H$, for the dissociation energy of H_2 is 4.747 eV, i.e. 458.0 kJ/mol. Comparing these two reactions $Pu + H_2 \rightarrow PuH_2$ and $Pu + H_2 \rightarrow PuH + H$ and using data of Tables 6 and 7, and Fig. 4, it is easy to see that the cross section of complex reaction is much bigger than that of exchange reaction. Therefore, complex PuH_2 will be formed promptly at rather low energy, which is in quite agreement with the practical situation.

3 Conclusion

In this work, the electronic ground states of PuH and PuH_2 with their structures have been respectively defined as $C_{\infty v}(X^8\Sigma)$ and $C_{2v}(\tilde{X}^7B_1)$ with the calculation by B3LYP/SDD method. The potential energy surface of PuH_2 derived from the many-body expansion theory obviously manifests no threshold in the reaction channel of $Pu(^7F_g) + H_2(X^1\Sigma_g^+)$.

Quasiclassical molecular reaction dynamics has been used to study the state-state process of $Pu(^7F_g) + H_2(X^1\Sigma_g^+)$. It is found that the reaction $Pu(^7F_g) + H_2(X^1\Sigma_g^+) \rightarrow PuH_2(\tilde{X}^7B_1)$ has no threshold in the lower kinetic energy, and the exchange reaction $Pu + H_2 \rightarrow PuH + H$ will occur when the kinetic energy is beyond 251 kJ/mol. However, the cross section of the exchange reaction is approximately one percent of the complex reaction. This agrees well with the fact of simultaneous hydrogenation of plutonium with the main product PuH_2, and is also coincident with the thermodynamic calculation[23].

Plutonium metal is extremely unstable under hydrogen atmosphere due to the transfer of 5f electron to hydrogen atom. The necessary condition for electron transfer is the variation of Gibbs function ΔG which is proportional to the difference of ionization between the donor and acceptor. For PuH, $I_d(Pu) - I_a(H) = 6.063 - 13.575 = -7.512$ eV $= -724.84$ kJ/mol, and for PuH_2 $I_d(Pu) - I_a(H_2) = 6.063 - 15.4259 = -9.3629$ eV $= -903.43$ kJ/mol, both are quite possible in thermodynamics. Because the sufficient condition is determined by the rate constant of electron transfer, it can be calculated by the one-electron model[24]. The present work has proved that there is no threshold for complex reaction.

In comparison with the hydrogenation process of common metals, the property of plutonium hydrides is very special, therefore to prevent the corrosion of plutonium is of great importance.

References

1 Kollár J., Vitos L. and Skriver H. L. Anomalous atomic volume of α-Pu. Phys. Rev. B, 1997, 55: 15353—15355.

2 Söderlind P., Wills J. M., Johansson B. et al. Structural properties of plutonium from first-principle theory. Phys. Rev. B, 1997, 55: 1997—2004.

3 Eisenstein J. C. Use of f orbitals in covalent bonding. J. Chem. Phys., 1956, 25: 142—146.

4 Martin W. C., Hagan L., Reader J. et al. Ground levels and ionization potentials for lanthanide and actinide atoms and ions. J. Phys. Chem. Ref. Data, 1974, 3: 771—779.
5 Li Q., Zhu Z. H., Wang H. Y. et al. Potential energy function for PuO^{2+}, PuH^{2+} and PuN^{2+} ions. J. Mol. Struct., 2002, 578: 177—180.
6 Larson D. T. and Haschke J. M. Characterization of plutonium oxides and oxide carbide. Inorg. Chem., 1981, 20: 1945—1950.
7 Haschke J. M., Allen T. H. and Morales L. A. Surface and corrosion chemistry of plutonium, Los Alamose Science, 2000, 26: 252—261.
8 Germain J. E. (Translators: Zheng S.A. and Gao Z.) Heterogeneous Catalysis. Shanghai: Shanghai Science and Technology Press, 1963, 84—85.
9 Meng D.Q., Jiang G., Liu X. Y. et al. The structure and potential energy function for Pu_3 system. Acta Physica Sinica (in Chinese), 2001, 50: 1268—1272.
10 Meng D. Q., Zhu Z. H. and Jiang G. Geometrical configurations of Pu_4 and the Jahn-Teller effect. J. Mol. Struct., 2002, 610: 241—245.
11 Hohenberg P. and Kohn W. Inhomogenous electron gas. Phys. Rev. B, 1964, 136: 864—871.
12 Hay P. J. and Martin R. L. Theoretical studies of the structures and vibrational frequencies of actinide compounds using relativistic effective core potentials with Hartree-Fock and density functional methods: UF_6, NpF_6, and PuF_6. J. Chem. Phys., 1998, 109: 3875—3881.
13 Becke A. D. Density-functional exchange-energy approximation with correct asymptotic behavior. Phys. Rev., 1988, 38: 3098—3100.
14 Perdew J. P. and Wang Y. Accurate and simple analytic representation of the electron-gas correlation energy. Phys. Rev. B, 1992, 45: 13244—13249.
15 Becke A. D. Density functional thermochemistry III. The role of exact exchange. J. Chem. Phys., 1993b, 98: 5648—5652.
16 Frisch M. J., Trucks G. W., Schlegel H. B. et al. Gaussian 98. Pittsburgh: Gaussian Inc, 1998.
17 Zhu Z. H. and Yu H. G. Molecular Structure and Molecular Potential Energy Function (in Chinese). Beijing: Science Press, 1997, 125—161.
18 Gao T., Wang Y. H., Jiang G. et al. Molecular structure and spectra of PuH and PuH_2. Nuclear Physical Review (in Chinese), 2002, 19: 13—16.
19 Murrell J. N., Carter S., Farantos S. C. et al. Molecular Potential Energy Functions. Chichester. New York. Brisbane. Toronto. Singapore: John Wiley and Sons, 1984, 29—33.
20 Yu S. Q. Micro-Chemical Reaction (in Chinese). Hefei: Anhui Science and Technology Press, 1985, 1—65.
21 Levine R. D. and Bernstein R. B. Molecular Reaction Dynamics. New York: Oxford University Press, 1974, 1—122.
22 Zhu Z. H. Atomic and Molecular Reaction Statics (in Chinese). Beijing: Science Press, 1996, 69—79.
23 Zou L. X., Sun I., Xue W. D. et al. Calculation of thermodynamic equilibrium for reactions of plutonium with air. Chinese Journal of Atomic and Molecular Physics (in Chinese), 2000, 17: 459—464.
24 Schatz G. C. and Ratner M. A. Quantum Mechanics in Chemistry. Englewood Cliffs, New Jersey: Prentice Hall, 1993, 234—246.